

# Experimental Validation of Standards Compliant Inductive Wireless EV Charging Station with Misalignments and Installation Dependent Performance

**Surasak Yousawat<sup>1</sup>, Ekkachai Chaidee<sup>2</sup>, Wuttikai Tammawan<sup>2</sup>, Thanet Sriprom<sup>1</sup>,  
Worrajak Muangjai<sup>1</sup>, Nopporn Patcharaprakiti<sup>1</sup>,  
Jutturit Thongpron<sup>1</sup>, and Anon Namin<sup>1†</sup>, Non-members**

## ABSTRACT

This paper presents the design, implementation, and evaluation of a prototype inductive wireless power transfer (IPT) system for electric vehicle (EV) charging stations, developed to comply with international standards of IEC 61980-1 and SAE J2954. The system was tested under various coil misalignment conditions (in x, y, and z axes) and three installation configurations—on-ground, in-ground, and underground—to assess its performance and feasibility for practical deployment as a charging station.

Experimental results demonstrate that the IPT system delivers a maximum power output of 11.2 kW, with IPT's efficiency reaching 90% and the DC-to-DC overall system efficiency at 87% during high-current operation of 70 A. The prototype maintained stable performance under realistic misalignment conditions of up to  $\pm 160$  mm in both lateral and longitudinal directions. In charging tests, the system successfully charged an EV battery from 40% to 95% state of charge within 110 minutes, while supplying power to both the battery and auxiliary loads.

These findings confirm the technical feasibility and reliability of the proposed IPT-based EV charging station. The system satisfies key requirements of the referenced standards and demonstrates strong potential for implementation in Thailand's emerging EV charging infrastructure.

**Keywords:** Inductive power transfer, Misalignment, Wireless EV charging, Wireless EV charging station, Infrastructure, Installation, Standards

Manuscript received on August 15, 2025; revised on September 17, 2025; accepted on October 2, 2025. This paper was recommended by Associate Editor Chainarin Ekkaravarodom.

<sup>1</sup>The authors are with Department of Electrical Engineering, Faculty of Engineering, Rajamangala University of Technology Lanna, Chiang Mai, Thailand

<sup>2</sup>The authors are with Department of Electrical Engineering, Faculty of Engineering, Rajamangala University of Technology Lanna, Chiang Rai, Thailand.

<sup>†</sup>Corresponding author: anamin@rmutl.ac.th

©2025 Author(s). This work is licensed under a Creative Commons Attribution-NonCommercial-NoDerivs 4.0 License. To view a copy of this license visit: <https://creativecommons.org/licenses/by-nc-nd/4.0/>.

Digital Object Identifier: 10.37936/ecti-eec.2525233.260855

## 1. INTRODUCTION

Climate change, primarily caused by greenhouse gas emissions from the burning of fossil fuels, is significantly impacting global temperatures and increasing the frequency and severity of natural disasters, such as droughts and floods [1][2]. The transportation sector alone accounts for nearly one-third of global energy demand and more than 20% of carbon emissions, necessitating a shift to electric and intelligent transportation systems to increase efficiency and reduce emissions [2][3].

The promotion of electric vehicles (EVs) is increasingly being recognized as a key strategy for reducing carbon emissions, achieving sustainability goals, and reaching net-zero targets. EVs offer significant advantages in reducing reliance on fossil fuels and compatibility with renewable energy sources [4][5]. However, challenges such as charging infrastructure, long charging times, and range concerns have hindered widespread adoption.

The development of electric vehicle (EV) charging stations is crucial to facilitating the transition to widespread EV adoption, with three main charging technologies being AC charging, DC fast charging, and wireless charging [6]-[8]. Although wireless charging is still emerging, it offers convenience without the need for a physical connection, making it attractive for urban environments and shared spaces [7]. Wireless Power Transfer (WPT) technology is emerging as a key solution for EV charging, leveraging magnetic induction coupling to facilitate power transfer without a physical connection. This technology enhances convenience and safety while supporting autonomous systems such as driverless vehicles and innovative parking solutions [9].

Additionally, integrating data communications capabilities into WPT systems can enhance functionality, enabling measured power and data transmission, thus addressing range and operational efficiency limits [10].

Standards govern WPT technology for EVs, the most significant of which are the SAE J2954 and the IEC 61980-1 [11][12]. These standards specify key parameters such as power levels (WPT1 at 3.7 kW, WPT2 at 7.7 kW, and WPT3 at 11 kW), coils' dimensions, and magnetic field safety limits to ensure compatibility and efficiency across a wide range of applications. The standards also

address the issue of coil misalignment, which can affect self-inductance and overall efficiency, emphasizing the significance of optimal ferromagnetic material placement [13]. Other relevant standards include ISO 15118 for EV communication and charging stations, and CISPR 11 for electromagnetic interference, all of which contribute to the reliability and safety of WPT systems in a variety of environments [14].

Previous research has proposed single-sided control, which simplifies the vehicle's hardware, supports coil offset, and achieves safe and efficient charging that complies with the criteria outlined in the SAE J2954 standard. Still, there are no system design or testing requirements to comply with the standard [15].

The performance of WPT systems has been evaluated under the criteria of coil spacing and offset; for example, [16] proposed a coil design that can withstand high offset, presented a rectangular and DD coil design [17], and [18] and [19] studied the effect of magnetic fields on the human body based on ICNIRP and IEEE C95.1 criteria, showing that when parallel or multiple coils are arranged (parallel WPT systems), the induced field values may exceed the safety limits if no proper control design is designed.

In addition, research has determined the operating frequency range, coils spacing, and acceptable offset values, under the requirements of SAE J2954 [20], in conjunction with the maintenance of the load voltage for dynamic EV charging [21], and the presentation of the battery charging current control technique in the wireless charging system for electric vehicles using the primary side control method only [22], most of the tests are still prototypes with low power. For the research, a high-power wireless charging system based on the SAE J2954 WPT Class 2 specification at 7 kW under acceptable misalignment conditions ( $\pm 75$ –100 mm) for battery charging has been presented by [23].

However, it was found that most research still focuses on testing in situations with perfect alignment. Studies focusing on field testing of WPT charging stations under misalignment conditions, according to the standards, are still limited. This work focuses on developing and experimentally validating the performance of wireless electric vehicle charging stations under conditions of imperfect coil alignment, referencing and complying with international standards criteria, to support the assessment of system readiness planned for practical applications in Thailand's industrial sector.

## 2. INDUCTIVE WIRELESS POWER TRANSFER ELECTRIC VEHICLES CHARGING STATION

WPT EV charging station technology can be divided into four types, which are (a) the Inductive power transfer (IPT), (b) the Capacitive power transfer (CPT), (c) the Microwave power transfer, and (d) the Infrared power transfer as specified in the IEC61980-1 standard [12]. This study focuses on the IPT that inductively transfers energy through the magnetic field. The IPT operates as a range

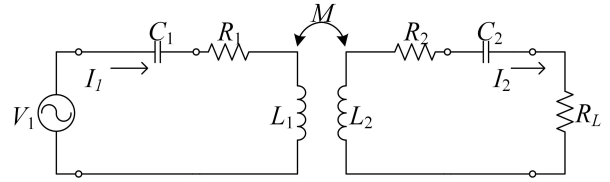


Fig. 1: Equivalent Circuit of the IPT coils [24][25].

of high-frequency high air-gap transformer for a wireless EV charging station.

This section presents the positions of the primary and secondary coils, defined with the distance  $z$ , the misalignment in the direction to forward of  $x$ , and the misalignment in the transverse to leftward of  $y$ , which is determined by the IEC 61980-1 standards [12].

The magnetic linkage between the primary and secondary coils is parametric by the coupling coefficient ( $k$ ). The mutual inductance ( $M$ ) between the primary and secondary coils, previously proposed for the analysis of a 10 kW IPT prototype [24] and extended in this work, is defined by Eq. (1) [24].

$$M_{(x,y,z)} = k_{(x,y,z)} \sqrt{L_1 L_2} \quad (1)$$

The equivalent circuit of the IPT is shown in Fig. 1. Indeed, the transmitter ( $Tx$ ), which is the primary of the IPT, consists of the resonant capacitor ( $C_1$ ), the primary parasitic resistance ( $R_1$ ), the primary leakage reactance ( $L_1$ ), and the mutual inductance ( $M_{12}$ ). Similarly, the receiver ( $Rx$ ) consists of the secondary resonant capacitor ( $C_2$ ), the secondary parasitic resistance ( $R_2$ ), the secondary leakage reactance ( $L_2$ ), and the secondary mutual inductance ( $M_{21}$ ). The relationship of the  $M$  is equal to the  $M_{12}$  and  $M_{21}$ , as shown in Eq. (2) and Fig. 1.[24]

$$M_{(x,y,z)} = M_{12(x,y,z)} = M_{21(x,y,z)} \quad (2)$$

When the IPT is supplied by the input voltage ( $V_1$ ) and the angular frequency ( $\omega$ ) source, the IPT must operate in the resonant conditions using  $C_1$  and  $C_2$ , which can be calculated using Eq. (3) [24][25].

$$C_1 = \frac{1}{\omega^2 L_1}, C_2 = \frac{1}{\omega^2 L_2} \quad (3)$$

The primary current ( $I_1$ ) and secondary current ( $I_2$ ) of the IPT can be derived as shown in the Eqs. (4) and (5).

$$I_1 = \frac{V_1 Z_2}{Z_1 Z_2 + (\omega M_{(x,y,z)})^2} \quad (4)$$

$$I_2 = \frac{j \omega M V_1}{Z_1 Z_2 + (\omega M_{(x,y,z)})^2} \quad (5)$$

From Fig. 1, the input power of the IPT is shown in Eq. (6), the output power is shown in Eq. (7), and the IPT

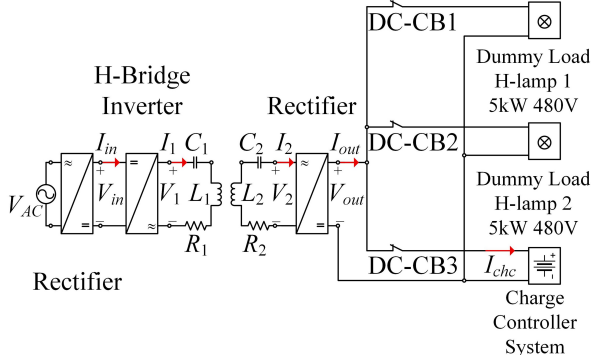


**Fig. 2:** Building Block of the Wireless Power Transfer System for the EV Charging Station.

**Table 1:** SAE J2954/1 WPT Power Class [11].

WPT Power Class	Maximum input VA	Minimum Target efficiency	Minimum target efficiency at offset position
WPT1	3.7 kVA	>85%	>80%
WPT2	7.7 kVA	>85%	>80%
WPT3	11.1kVA	>85%	>80%
WPT4	22 kVA	TBD	TBD

efficiency is calculated by using Eq. (8) [24][25].

$$P_1 = \frac{[R_1(R_2 + R_L)^2 + (\omega M_{(x,y,z)})^2(R_2 + R_L) + X_2^2 R_1] V_1^2}{[R_1(R_2 + R_L) - X_2 X_1 + (\omega M_{(x,y,z)})^2]^2 + [X_2 R_1 + X_1(R_2 + R_L)]^2} \quad (6)$$

$$P_2 = \frac{(\omega M_{(x,y,z)}) V_1^2 R_L}{[R_1(R_2 + R_L) - X_2 X_1 + (\omega M_{(x,y,z)})^2]^2 + [X_2 R_1 + X_1(R_2 + R_L)]^2} \quad (7)$$

$$\eta_{IPT} = \frac{(\omega M_{(x,y,z)})^2 R_L}{[R_1[(R_2 + R_L)^2 + X_2^2] + (\omega M_{(x,y,z)})^2(R_2 + R_L)]} \quad (8)$$

Equations (1) to (8) were derived to describe the circuit parameters of the IPT coils. From the IPT constructions, the magnetic coupling under high-frequency resonant conditions, the output power, and the efficiency of the IPT coils can be evaluated using Eqs. (7) and (8) [24].

Equation (8) describes the effect of output resistive load, the square of frequency, mutual impedance, and the IPT circuit impedance parameters. The maximum conditions of the IPT coils or coil-to-coil efficiency, or those values, may be derived from the derivatives of this equation concerning the derivatives of those IPT circuit parameters [24][25].

## 2.1 General System Requirement of the Wireless EV Charging Station System [11][12]

The WPT system for EVs, as defined by the SAE J2954 [11] and the IEC 61980-1 [12] standards, comprises two

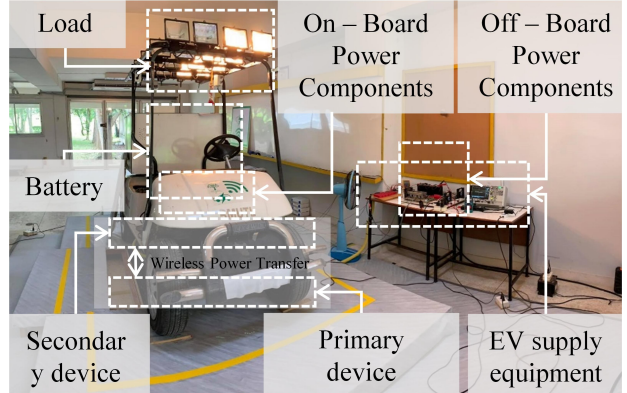


**Fig. 3:** The Prototype Wireless EV Charging Station.

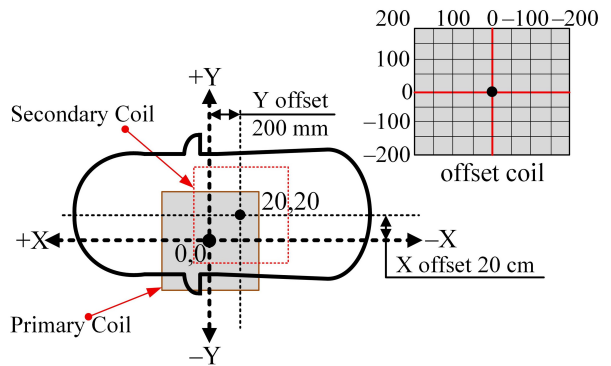


**Fig. 4:** Offset Positions (Adapted from [12]).

**Table 2:** SAE J2954 Specification of the Z-Classes and the Misalignment Distance [11].

Specification of the Z-Class	Ground clearance Range (mm) between primary and secondary coil
Z1	100 – 150
Z2	140 – 210
Z3	170 – 250
Offset direction	Misalignment Distance
$\Delta X$	$\pm 75$
$\Delta Y$	$\pm 100$
$\Delta Z$	$Z_{\text{nom}} - \Delta_{\text{low}} - \Delta_{\text{high}}$
Rotation, Roll, and Yaw	Testing at $\pm 2, 4$ and 6 degrees

main subsystems: the supply device and the EV device. Electrical energy is transferred wirelessly via electromagnetic fields between the primary device (located on the supply side) and the secondary device (located on the vehicle side). The key components on the supply side include the off-board power components, while the EV side consists of the on-board power components, the traction battery, and the electrical load. The WPT system configuration is illustrated in Fig. 2, which presents the prototype of a wireless EV charging station.

According to the SAE J2954 standards [11], wireless

charging systems are classified into four power levels. WPT1 is intended for residential use with a maximum power capacity of 3.7 kW from a single-phase 120 V AC supply. WPT2 supports higher power up to 7.7 kW from a 240 V AC supply. WPT3 increases the power to 11.1 kW, while WPT4 supports up to 22 kW from a three-phase 380 V AC supply or medium-voltage sources. For all charging levels, the wireless power transfer (WPT) system must achieve a minimum efficiency of 85% for matched systems and at least 80% for interoperable systems.

## 2.2 Measurement Convention of Offset

The misalignment testing of the WPT system is conducted to evaluate the efficiency and output power performance under constant input voltage conditions.

In this test, the relative positions between the primary and secondary devices are intentionally shifted along the x, y, and z axes by the definitions provided in IEC 61980-1, specifically Clause 8.3 on Measurement Orientation and Subclause 8.3.2 on Orientation [12]. The measurement setup is illustrated in Fig. 4.

The alignment between the primary and secondary coils has a significant impact on system efficiency. As shown in Fig. 4, the positional relationship between the coils can be described using offset parameters defined in IEC 61980-1 [12].

**Lateral Offset ( $\Delta X$ ):** Horizontal displacement perpendicular to the vehicle's longitudinal axis. This represents side-to-side misalignment between the primary and secondary coils.

**Longitudinal Offset ( $\Delta Y$ ):** Horizontal displacement parallel to the vehicle's longitudinal axis, corresponding to forward or backward misalignment.

**Vertical Gap ( $\Delta Z$ ):** Distance between the coil surfaces (mechanical air gap), which is determined by the mounting height and vehicle ground clearance.

In Fig. 4, the shaded gray areas represent the physical footprints of the *Tx* and *Rx* coils, while the dashed lines indicate the offset limits considered in testing (e.g.,  $\pm 20$  mm in both  $\Delta X$  and  $\Delta Y$ ). These parameters are critical for validating performance under parking conditions. By evaluating efficiency and coupling at different offsets, the design can ensure compliance with the IEC 61980-1 standards requirements for misalignment tolerance.

The distance between the *Tx* and *Rx* coils, referred to as the magnetic gap, is categorized according to the Z-classes, as shown in Table 2. Figs. 4 through 6 illustrate additional information on coil misalignment in various directions and positions. Further details are provided in Table 2, which indicates that the vehicle ground clearance depends on the type of vehicle, ranging from 160 mm for small passenger cars to over 200 mm for SUVs [11].

The effect of coils misalignment on the performance of a WPT system was evaluated based on Eq. (1), following the requirements specified in SAE J2954 standard for the design of WPT systems used in EVs. The ground clearance between the primary and secondary coils

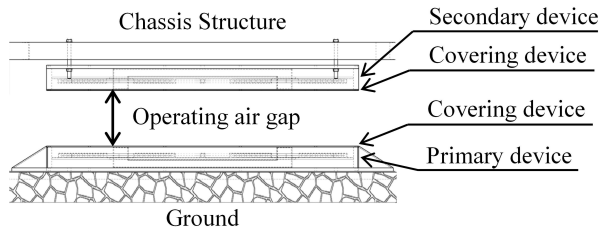


**Fig. 5:** Offset Positions for On-Ground Mounting (Adapted from [11, 12]).

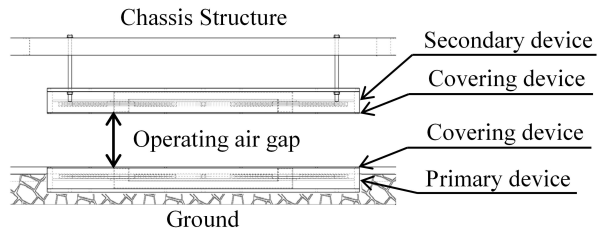


**Fig. 6:** Offset Positions for In-Ground Mounting (Adapted from [11, 12]).

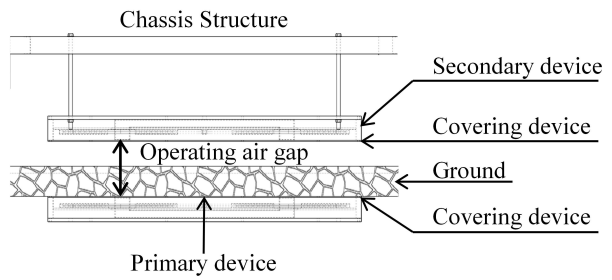


**Fig. 7:** Offset Positions for Under-Ground Mounting (Adapted from [12]).

is defined according to Z-Class categories, where Z2 corresponds to a clearance range of 140–210 mm. For planar misalignment testing, the offset distances in the X and Y axes are set to  $\pm 75$  mm and  $\pm 100$  mm, respectively. In the case of Z-axis misalignment, the position varies from the nominal coil distance ( $Z_{\text{nom}}$ ) by reducing it with  $\Delta_{\text{low}}$  and increasing it with  $\Delta_{\text{high}}$ , within a range of 20 mm to 300 mm, as defined in the standard.

## 2.3 Primary Device Mounting

The developed wireless power transfer (WPT) system can be installed by the IEC 61980 and the SAE J2954 standards in three configurations: (1) on-ground installation, (2) in-ground installation, and (3) underground installation [11][12].

To evaluate the performance of the WPT system under different installation scenarios, it is essential to investigate the impact of misalignment on the system's power transfer characteristics for each configuration.

The primary coil of an IPT-based EV charging station can be installed using several mounting configurations,

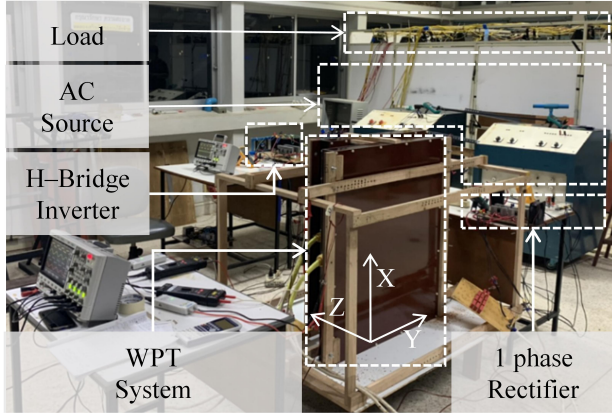


**Fig. 8:** Experimental Setup of XYZ-axis misalignment of the Wireless EV Charging System.

each with distinct implications for electromagnetic coupling, installation complexity, and durability. Figs. 4 to 6 illustrate three representative mounting approaches:

**On-ground mounting** is illustrated in Fig. 5. In this configuration, the primary device is positioned directly on the ground surface and protected by a covering device.

*Advantages:* Simplified installation with minimal civil works; straightforward maintenance access.

*Limitations:* Greater exposure to mechanical damage, debris accumulation, and potential flooding; may require robust weatherproof enclosures.

**In-ground mounting**, as shown in Fig. 6, features the primary device embedded flush with the ground surface, with the covering device forming part of the pavement.

*Advantages:* Reduced obstruction to vehicles and pedestrians; lower risk of physical impact compared to on-ground mounting.

*Limitations:* Requires moderate civil works; careful sealing and drainage design to prevent water ingress; installation and replacement may be more time-consuming.

**Underground mounting** is shown in Fig. 7. The primary device is installed beneath the ground surface with an additional covering device placed above a protective structural layer.

*Advantages:* Maximum protection from environmental exposure and physical damage; improved safety.

*Limitations:* An increased vertical gap ( $\Delta Z$ ) between coils can reduce coupling efficiency. Additionally, installation and maintenance require more extensive civil engineering work.

The choice of mounting method should be based on site factors, vehicle type, parking space design, environmental conditions, maintenance accessibility, and compliance with IEC 61980 safety and performance requirements.

### 3. EXPERIMENTS

The experimental validation of a standards-compliant wireless EV charging station, with performance depen-

dent on misalignment and installation, was set up and tested as follows.

Firstly, the 10 kW IPT prototype uses six block-UU EE55 ferrite cores ( $330 \times 520 \times 20$  mm) with a 160 mm air gap. The primary and secondary coils have 18 turns of homemade Litz wire (41 strands, 18 SWG, cotton-insulated), which was constructed and evaluated as previously published [24], and was prepared for testing.

Secondly, the IPT coils were set up for performance testing and evaluation under various misalignment conditions. Thirdly, misalignment-dependent performances were evaluated under varying installation configurations, and experiments were conducted. Finally, a prototype wireless EV charging station was measured to determine its performance. The tests were specified in accordance with the IEC 61980-1 and SAE J2954 standards, as follows.

#### 3.1 Misalignment-Dependent Performance Testing of the IPT System

This experiment aims to investigate the effects of IPT coil misalignments on their output performance, which was experimentally studied by varying misalignment conditions along the x, y, and z axes, as shown in Fig. 4 and Fig. 8. The experimental procedure for testing the misalignment-dependent performance of the IPT system is as follows.

Firstly, the misalignment was configured in the x-y plane, representing forward-backward and lateral offsets.

Secondly, the WPT system operated under a constant load using a 10kW halogen lamp at a frequency of 31.4 kHz with a fixed input voltage of 100 V throughout the experiment.

In the prototype, the inverter operating frequency of the IPT coils was lower than the requirements of the IEC 61980-1 and SAE J2954 standards [11][12], primarily due to the absence of high-frequency power switches and drivers during the early research stage. Nonetheless, adherence to these standards is recommended for future corrective requirements.

Thirdly, the vertical gap between the primary and secondary coils was defined according to the SAE J2954 standards. Also, the misalignment was varied incrementally by 20 mm, ranging from 0 to 160 mm along the x, y, and z axes. For tests involving misalignment in the x and y directions, the z-axis distance was held constant at 160 mm.

Finally, the experimental results were analyzed to evaluate the power transfer capability and system efficiency under various offset conditions.

#### 3.2 Misalignment and Installation Configurations – Dependent Performance of the Wireless EV Charging Stations

The misalignment-dependent performance of wireless EV charging stations, installed according to the SAE

J2954 and IEC 61980-1 standards, was evaluated in three configurations: on-ground, in-ground, and underground. To assess the system's performance under each installation scenario, the effect of misalignment on system efficiency was investigated under the condition where the vertical distance (z-axis) between the primary and secondary coils was fixed at 160 mm, as shown Fig. 9.

Misalignments were introduced along the x- and y-axes, ranging from  $-200$  mm to  $+200$  mm, with a grid resolution of 50 mm, resulting in 81 discrete test points. A laser-guided alignment system was employed to ensure precise positioning at each misalignment point. During testing, the input voltage was set at 373.5 V, with a constant resistive load applied. At the reference position (0, 0), the measured current was 35.98 A. These tests enabled systematic observation of the system behaviour under various misalignment conditions and provided a clear comparison of performance across the different installation types.

Fig. 10 shows the system-level power-flow diagram with tap points used to evaluate WPT performance. Power flows from the AC input ( $V_{AC}$ ) to the rectified DC ( $V_{in}$ ,  $I_{in}$ ,  $P_{in}$ ), through the H-Bridge inverter ( $V_1$ ,  $I_1$ ,  $P_1$ ), and the LC filter ( $L_1$ ,  $C_1$ ). It is then wirelessly transferred, measured at ( $V_2$ ,  $I_2$ ,  $P_2$ ), rectified again, and delivered to the load ( $V_{out}$ ,  $I_{out}$ ,  $P_{out}$ ). These tap points enable assessment of efficiency, stability, and overall system performance.

### 3.3 Performance of a Prototype Wireless EV Charging Station

The performance of a prototype wireless EV charging station was evaluated under charging conditions for an EV battery with a total capacity of 10 kWh. The charging capacity rate was set at 0.5 C, corresponding to a maximum allowable charging power of 5 kW. The system was equipped with a charge controller and a battery management system (BMS) to regulate and manage the charge/discharge processes. Since the WPT system was designed for a 10 kW power level, an additional external dummy load was connected in parallel to simulate the dynamic load behavior of a vehicle and ensure full system loading, as shown in Fig. 9.

To evaluate the high-current wireless charging performance, the test was conducted at a constant current of 70 A following a structured procedure. The battery was first discharged from a state of charge (SoC) of 95% down to 40%. Subsequently, the charge controller was configured to operate at a constant current of 70 A, while the dummy load was used to maintain the required voltage level for the controller to function correctly. Once stabilized, power from the WPT system was supplied to both the dummy load and the charge controller, initiating the battery charging process from SoC 40% up to 95%. Finally, the charging efficiency and behavior across the entire SoC range were analyzed to assess the system's capability under high-current operation conditions.

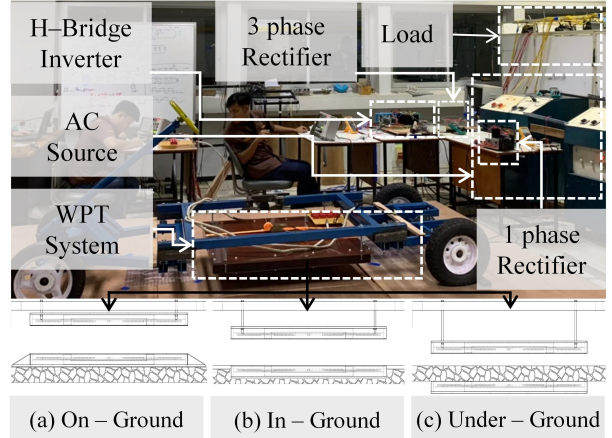


Fig. 9: Installation Testing of Wireless EV Charging Station.

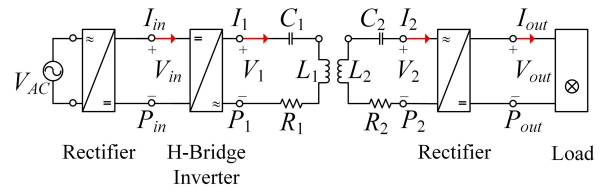


Fig. 10: WPT System Power Measurement Terminals.

## 4. RESULTS

The testing results of the Prototype of Inductive Wireless Power Transfer for EV Charging Station in Thailand include the  $M_{(x,y,z)}$  and  $k_{(x,y,z)}$  measurements, the offset test, which is transmitted to the WPT system to the components – Testing of Prototype Wireless Electric Vehicle Battery Charging Station system.

### 4.1 Misalignment Dependent Performance of IPT Coils

The simulation and measurement results of  $M(x, y, z)$  of the IPT coils at the offset positions along (0, 0, 200) mm to (0, 0, 300) mm with a step of 20 mm are shown in Fig. 11 (d) and Fig. 12 (d). The  $M(0, 0, 20)$  mm was 220 uH, then decreased along the position to  $M(0, 0, 60)$  mm due to the flux linkage and the flux leakage between  $Tx$  and  $Rx$ , changing the direction extremely. The  $M(0, 0, 8)$  mm to  $M(0, 0, 300)$  mm decrease slightly.

The  $M(x, y)$  of the IPT that was measured at the positions of the offset distance was performed under the condition that the z-axis distance was fixed at 160 mm, and the offset distance in the x and y axes was adjusted from 0 to 160 mm in increments of 20 mm each.

According to Figs. 11(c) and 12(c), the input current also increases with increased misalignment, posing a challenge for WPT systems. Specifically, the input current increased up to three times compared to the zero-offset condition. The maximum power output recorded was 1.29 kW, which is approximately 2.6 times higher than the nominal power at zero offset (0.5 kW).

The test results for forward misalignment along the

x-axis, as shown in Figs. 11(b) and 12(b) indicate that the output power increases with the offset distance. However, the system efficiency showed a slight variation, decreasing from 85% to 81%, as shown in Fig. 11 (a) and 12 (a).

In the case of lateral misalignment along the y-axis, the input current also increased with the offset, reaching a maximum of 10.8 A. The highest power output observed in this condition was 909.72 W with an efficiency of 84%. For vertical displacement along the z-axis, the output power was found to increase with increasing distance between coils. The maximum power output was 2.15 kW at a separation of 280 mm, which is more than four times higher than the power at the nominal 160 mm distance. Despite this, the highest efficiency of 84% was achieved at the nominal 160 mm gap, corresponding to an output power of 415.23 W.

The results from Figs. 11 and 12 indicate that the output power increases when misalignment occurs along the x, y, and z axes in a wireless power transfer (WPT) system. Misalignment typically reduces system efficiency and output power, but in this case, output power increases with misalignment in different axes.

The results indicate that misalignment impacts the mutual inductance between the coils, a key factor in energy transfer. The mutual inductance ( $M$ ) changes as misalignment occurs, which influences the primary current ( $I_1$ ) and secondary current ( $I_2$ ), as shown in Eqs. (4) and (5). By calculating the  $P_{in}$  and the  $P_{out}$  from Eqs. (6) and (7), it can be shown that the change of  $M$  affects the power transfer.

The increase in output power may be due to the mutual inductance ( $M$ ) changing with the eccentricity of the coil set, which increases the transferred power. In this case, the analysis from the equation can help explain how the eccentricity may change the characteristics of the mutual inductance, which directly affects the efficiency of the wireless power transmission system, as shown in Eq. (8).

#### 4.2 Installations Dependent Performance of IPT Coils

Based on the experimental results presented in Fig. 13 to Fig. 15, the performance of a 10 kW IPT coil prototype was evaluated under the effect of misalignment caused by variations in the parking position of the EVs. It was found that the misalignment between the Tx and the Rx coils significantly affects the output power and efficiency of the system.

For the On-ground installation, the system achieved a maximum output power of 10.2 kW and peak efficiency of 87% at the center position (0, 0). However, when the coils were misaligned to (-200, -200), the output dropped to a minimum of 1.2 kW, corresponding to a 52% efficiency.

Similar behavior was observed in the In-ground configuration, where the system delivered up to 10.62 kW with 87% efficiency at the center, but dropped to 827.78 W and 52% efficiency at the furthest misalignment.

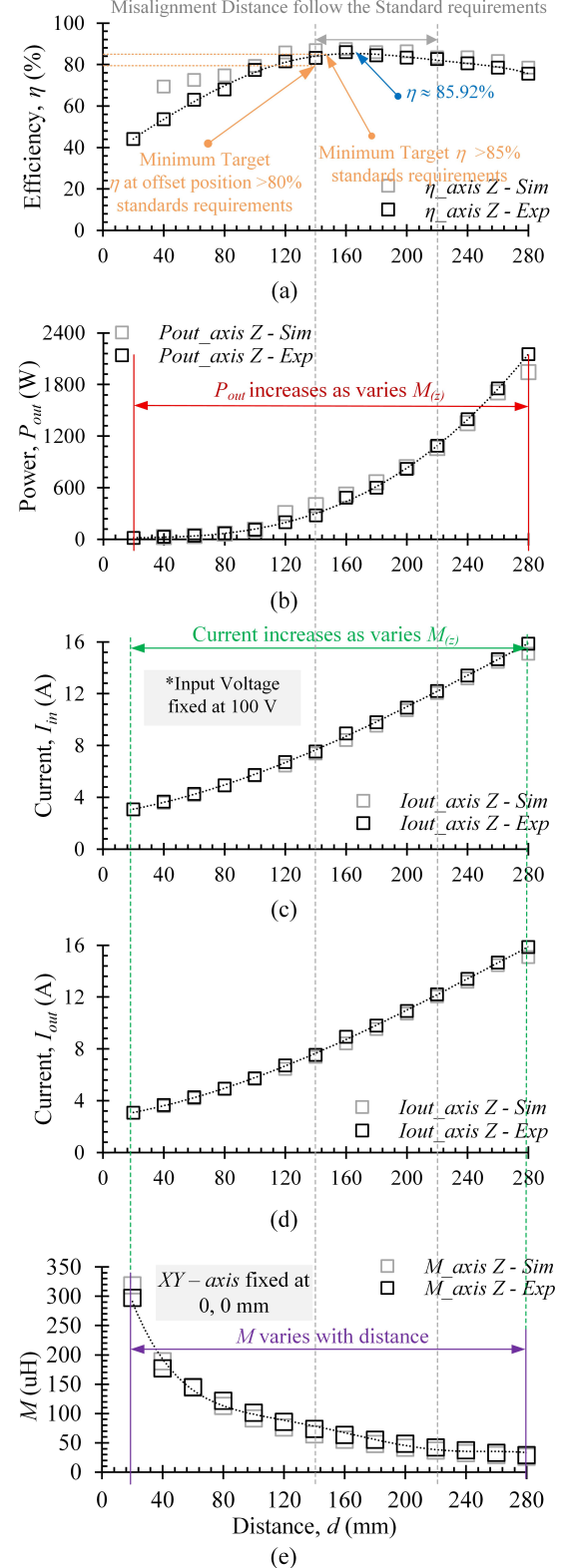


Fig. 11: Misalignment Performance of the IPT Coils ( $M_{(z)}$ ,  $P_{out(z)}$ ,  $I_{in(z)}$ ,  $I_{out(z)}$ ,  $\eta_{(z)}$ ).

The Under-ground installation yielded the highest performance, reaching 11.2 kW and 89% efficiency at the aligned position (0, 0), but also dropped significantly to

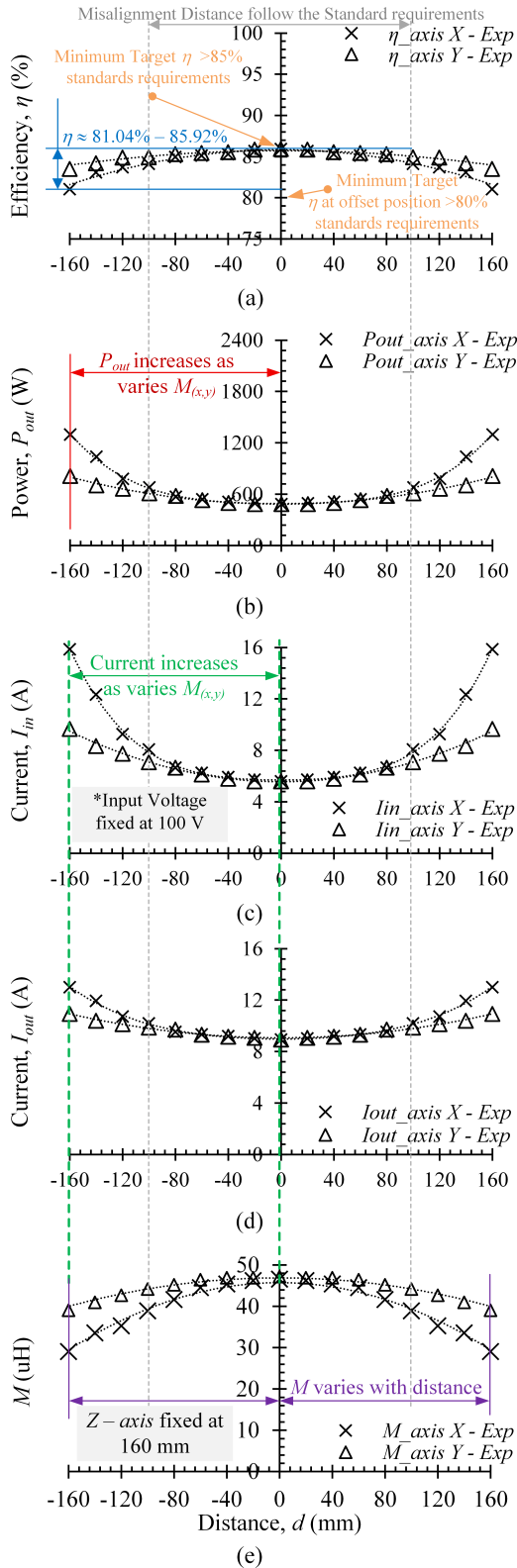


Fig. 12: Enlarged Image of the IPT Coils Performance ( $M_{(x,y)}$ ,  $P_{out(x,y)}$ ,  $I_{in(x,y)}$ ,  $I_{out(x,y)}$ ,  $\eta_{(x,y)}$ ).

1.38 kW and 57% at (-200, -200).

The findings underscore the crucial role of coil alignment in ensuring optimal system performance. Under

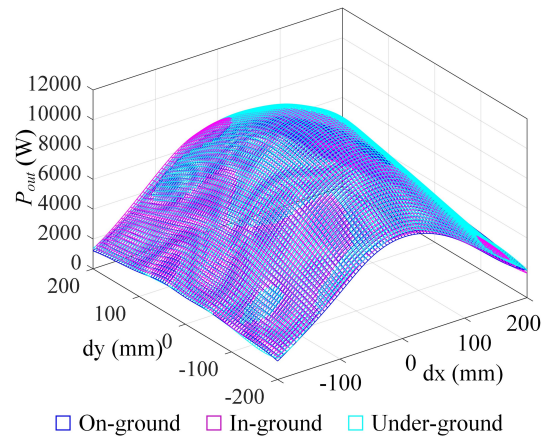


Fig. 13: Output Power – Misalignment Characteristics of WPT Installations.

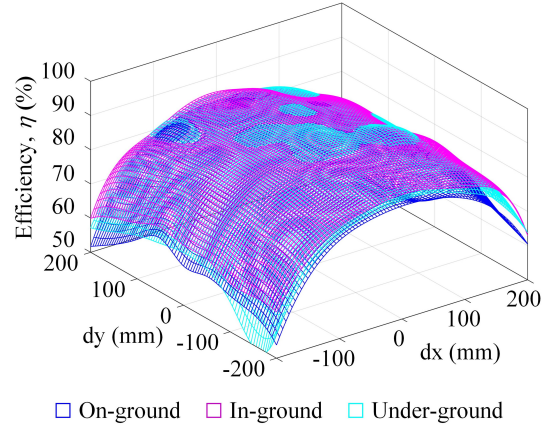


Fig. 14: Misalignment Characteristics of WPT Installations.

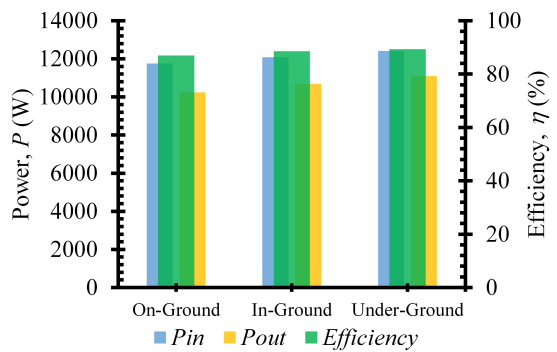
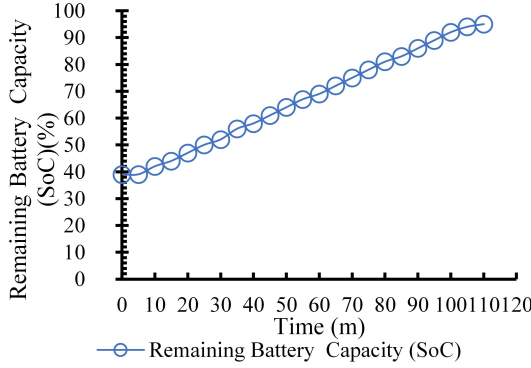


Fig. 15: Comparison of the Output Power and Efficiency of the Different WPT Installations.

all three installation types, the system maintained acceptable performance within a misalignment range of  $\pm 50$  mm in the longitudinal direction (x-axis) and  $\pm 100$  mm in the lateral direction (y-axis). These tolerances are considered practical for real-world applications.

From the comparative analysis shown in Figs. from



**Fig. 16:** Logged SoC Characteristics of the EV Battery during Wireless CC Charging of 70 A.

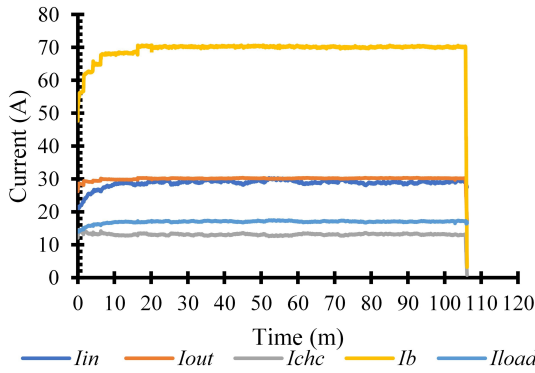


**Fig. 17:** Charging Current Characteristics of the system versus time during the 70 A wireless charging test.

13 to 15, it can be concluded that despite differences in installations, On-ground, In-ground, and Under-ground, the WPT system demonstrated relatively consistent performance. As shown in Fig. 15, the overall efficiency across the three configurations remained within a narrow range of 87% to 89%, suggesting that all installation methods are viable for effective battery charging in electric vehicles.

Therefore, the output power and efficiency of the IPT coils for On-ground, In-ground, and Underground installations are not significantly different.

#### 4.3 Charging Performance of a Prototype Wireless EV Charging Station

The result of wireless EV charging at a rated current of 70 A is illustrated in Fig. 16. From the experimentally logged data, the battery's SoC increased from 40% to 95% under a constant current charging of 70 A. The total charging duration required to reach the target SoC was 110 minutes.

Figure 17 illustrates the logged profile of the charging current at a rated current of 70 A. The measured values are in direct current (DC), including the input current ( $I_{in}$ ), output current ( $I_{out}$ ), current supplied to the charging control system ( $I_{chc}$ ), charging current of the battery ( $I_b$ ), and the current delivered to the auxiliary

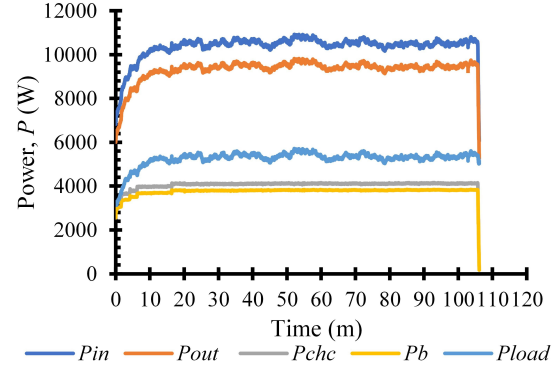


**Fig. 18:** Output Power Characteristics of the Wireless EV Charging System during a 70 A Charging Tested.

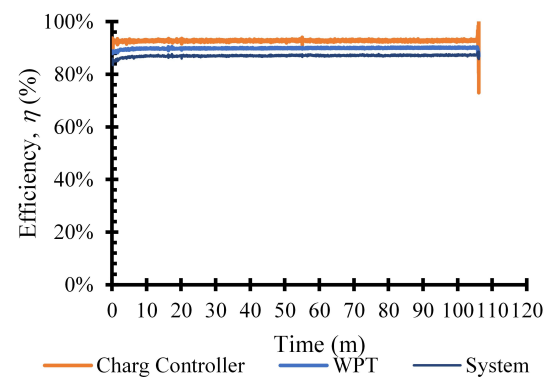


**Fig. 19:** The Wireless EV Charging System Efficiency Characteristics of the 70 A Charging Tested.

load ( $I_{load}$ ). It is observed that the sum of  $I_{load}$  and  $I_{chc}$  is equal to the  $I_{out}$ .

Figure 18 shows the output power characteristics measured during the wireless charging station test at a rated current of 70 A. The power values consist of input power ( $P_{in}$ ), output power ( $P_{out}$ ), power delivered to the charging control system ( $P_{chc}$ ), power used for battery charging ( $P_b$ ), and power delivered to the auxiliary load ( $P_{load}$ ). It should be noted that the total output power ( $P_{out}$ ) is the sum of the power supplied to the charging controller and the auxiliary load, i.e.,  $P_{out} = P_{chc} + P_{load}$ .

Figure 19 illustrates the system efficiency measured at a rated current of 70 A. The efficiencies can be divided into three components, which are the charging control system efficiency, the WPT system efficiency, and the overall system efficiency.

In the wireless EV charging station experiment at a constant current of 70 A, the charging procedure from SoC of 40% to 95% took a total duration of 110 minutes. During this process, the system delivered 3,814 W to the EV battery while supplying 5,567 W to an auxiliary load, resulting in a total system output power of 9,381 W.

The charging control unit exhibited an efficiency of 93%, while the WPT system demonstrated an efficiency of 90%. The overall system efficiency, calculated based on the total input power of 10,782 W, was 87%.

**Table 3:** Comparison to the IEC 61890-1 Standards [12] and the Benchmark Contributions.

Standard Testing Topics	This Paper	[15]	[17]	[19]	[21]	[23]
1 General system requirements	✓					
1.1 General	✓	⊗	⊗	✓	⊗	✓
1.2 Efficiency	✓	⊗	✓	✓	⊗	✓
1.3 Measurement convention	✓				⊗	
1.3.1 General	✓	⊗	⊗	⊗	⊗	✓
1.3.2 Orientation	✓	⊗	⊗	⊗	⊗	✓
1.3.3 Measurement convention of the parking space	✓	⊗	⊗	⊗	⊗	✓
1.3.4 Measurement convention of offset	✓	⊗	⊗	⊗	⊗	✓
1.3.5 Measurement convention of the primary device	✓	⊗	⊗	⊗	⊗	⊗
1.3.6 Distance between the primary and secondary device (mechanical air gap)	✓	✓	✓	✓	✓	✓
1.3.7 Primary device mounting	✓	⊗	⊗	⊗	⊗	⊗
1.3.8 In-ground-mounting	✓	⊗	⊗	⊗	⊗	⊗
1.3.9 On-ground-mounting	✓	✓	✓	✓	✓	✓
1.4 Primary and secondary device construction	✓	⊗	⊗	✓	✓	✓

✓ = Requirement met through testing and analysis  
⊗ = Not applicable or not evaluated in this study

These results confirmed the effectiveness of the proposed system architecture in maintaining high power transfer and energy conversion efficiency under high current operation.

## 5. DISCUSSIONS

This research developed and validated an inductive wireless EV charging station that adheres to IEC 61980-1 and SAE J2954 standards [11][12], designed explicitly for imperfect coil misalignments and various mounting setups.

The prototype achieved up to 11.2 kW, a peak IPT efficiency of approximately 90%, and a DC-to-DC efficiency of about 87% at 70 A. It demonstrated tolerance for lateral and longitudinal offsets of roughly  $\pm 160$  mm.

It charged a vehicle from a 40% to a 95% state of charge in approximately 110 minutes, indicating its practical readiness for high-power wireless charging applications in Thailand. Output power increased under certain misalignment conditions. Consistent with the equivalent-circuit model and Eqs. (1) to (8), power and efficiency depend on  $M(x, y, z)$  non-linearity and resonant conditions. By setting up the system impedances equal to the  $M(x, y, z)$ , the maximum power transfer can be controlled under various distances and misalignments, as published in [26].

Off-center positioning can alter edge flux and leakage paths, changing  $M$  and therefore  $I_1$  and  $I_2$ , which can increase  $P_{out}/P_{in}$ . However, input current also rises, and efficiency varies modestly (e.g., from ~85% to ~81%), implying the need for consideration of thermal and safety factors for continuous operation.

Table 3 provides a comparative summary between the SAE J2954 standards requirements [11] and the performance of this work. The prototype complies with the  $Z_2$  class requirement (with a coil gap of 160 mm, which falls within the defined 140–210 mm range) and demonstrates an expanded tolerance for coil

misalignment—up to  $\pm 160$  mm in both  $\Delta X$  and  $\Delta Y$  directions, exceeding the minimum testing thresholds outlined in the standards.

Additionally, the system delivers a peak power of 11.2 kW, which slightly surpasses the WPT3 class limit of 11.1 kW. It maintains a system efficiency between 81% and 89%, thereby satisfying both nominal and misaligned efficiency targets defined by the standards by more than 85% nominal and more than 80% under offset.

Table 5 shows that the developed IPT prototype meets IEC 61980-1 general requirements more extensively than earlier works. It satisfies key aspects such as resonant operation, Tx/Rx coil construction, mechanical air-gap alignment, offset measurement conventions, and three installation types (on-ground, in-ground, under-ground), demonstrating greater system completeness. This highlights the feasibility and scalability of the system for future EV wireless charging infrastructures. In contrast, most prior studies focused on ideal alignment and on-ground setups, lacking standardized testing protocols. Although [19] reported EMC compliance, both this and earlier studies have yet to fully evaluate communication, protection, and marking, underscoring areas for further research. The prototype, however, delivers WPT3-class power (~11.2 kW), a peak efficiency of approximately 90%, and robust tolerance to misalignment of up to  $\pm 160$  mm, exceeding the SAE J2954 thresholds. Overall, this work indicates higher deployment readiness than typical low-power prototypes, strengthening its value for standards-compliant and practical EV charging applications.

However, areas such as communication capability, electrical protection, electromagnetic compatibility (EMC), and labeling have not yet been fully evaluated in this study. These gaps indicate the need for further research and system improvements to ensure full compliance with the standards when testing facilities are available.

For future research, it is recommended to integrate a control charge communications system based on IEC 61980-2 [27]. Further investigations into electromagnetic compatibility, thermal protection, and environmental durability testing, aligned with CISPR 11 [28] and IEC 61980-3 [29] standards, are essential compliances.

In Thailand, pioneers in standard-compliant development, such as Li-ion battery pack design [30] and on-chip analog mixed-signal testing [31], are university professors who have taken on industrial challenges, a path this research aims to follow.

Nevertheless, the reviewed and evaluated wireless power transfer technologies for EVs in terms of efficiency and practical implementation of Inductive, Capacitive, and Hybrid WPT systems show that this is the initial stage of research and has been expanded to the industrial standards, the zero voltage or current switching of inverters, and the Power Balance control system development for EV wireless power transfer in Thailand [32][33][34].

This work demonstrates a standards-compliant inductive WPT prototype with high power, efficiency, and misalignment tolerance, indicating readiness for EV charging in Thailand. Future research will focus on communication, EMC, protection, and durability, while expanding to capacitive and hybrid systems. The study establishes a strong foundation for standard compliance and industrial deployment.

## 6. CONCLUSION

This study presents the development and evaluation of a prototype IPT system tailored for EV charging applications. The proposed system was tested under various coil misalignment conditions and installation configurations, strictly adhering to international standards, namely IEC 61980-1 and SAE J2954.

Experimental results confirmed the robustness and reliability of the system. Notably, the IPT coils achieved an efficiency of up to 90%, with a DC-to-DC overall system efficiency of 87% under high-current operation at 70 A. The prototype also demonstrated a maximum output power of 11.2 kW under optimal alignment, consistent with the WPT3 class specification. Notably, the system maintained acceptable performance under realistic misalignment of  $\pm 75$  mm in the longitudinal (x-axis) and  $\pm 100$  mm in the lateral (y-axis) directions, thereby satisfying practical deployment requirements.

Furthermore, all installations of on-ground, in-ground, and underground exhibited comparable performance, with system efficiency ranging between 87% and 89%.

In conclusion, the performance characteristics of the wireless EV charging station, including output power and efficiency, were not significantly affected by misalignments and installations.

These results confirm the feasibility and scalability of the proposed IPT system for future wireless EV charging station.

## ACKNOWLEDGEMENT

This work was initiated with support from the Development of Wireless Electric Vehicle Battery Charging Station project, funded by the Energy Conservation and Promotion Fund, Energy Policy and Planning Office (EPPO), Ministry of Energy, Thailand, under contract ENCONFUND 07-02-61-001/13.

Additionally, in partnership with Rajamangala University of Technology Lanna and the Education Development Program Fund, the project is titled "Start-up Development for Industrial Education in Electrical Engineering" under Grant RMUTL MHESI 0654.40/EE400/2025.

## REFERENCES

- [1] S. Bolan, et al., "Impacts of climate change on the fate of contaminants through extreme weather events," *Science of The Total Environment*, vol. 909, Jan. 2024, Art. no. 168388. doi: 10.1016/j.scitotenv.2023.168388.
- [2] P. Jeebklum and C. Sumpavakup, "Metamaterial Slabs for Electric Vehicle Wireless Charging Application," *IEEE Access*, vol. 12, pp. 156717-156729, 2024, doi: 10.1109/ACCESS.2024.3485180.
- [3] S. Fang, Z. Tian, C. J. Roberts, and R. Liao, "Guest Editorial: Special Section on Toward Low Carbon Industrial and Social Economy of Energy-Transportation Nexus," *IEEE Transactions on Industrial Informatics*, vol. 18, pp. 8146-8148, Nov. 2022, doi: 10.1109/TII.2022.3185294.
- [4] S. P. Sathiyan et al., "Comprehensive Assessment of Electric Vehicle Development, Deployment, and Policy Initiatives to Reduce GHG Emissions: Opportunities and Challenges," *IEEE Access*, vol. 10, pp. 53614-53639, 2022, doi: 10.1109/ACCESS.2022.3175585.
- [5] U. Fesl and M. B. Özdemir, "Electric Vehicles: A Comprehensive Review of Technologies, Integration, Adoption, and Optimization," *IEEE Access*, p. 1, Jan. 2024, doi: 10.1109/access.2024.3469054.
- [6] S. S. G. Acharige, M. E. Haque, M. T. Arif, N. Hosseinzadeh, K. N. Hasan, and A. M. T. Oo, "Review of Electric Vehicle Charging Technologies, Standards, Architectures, and Converter Configurations," *IEEE Access*, vol. 11, pp. 41218-41255, 2023, doi: 10.1109/ACCESS.2023.3267164.
- [7] S. A. Q. Mohammed and J.-W. Jung, "A Comprehensive State-of-the-Art Review of Wired/Wireless Charging Technologies for Battery Electric Vehicles: Classification/Common Topologies/Future Research Issues," *IEEE Access*, vol. 9, pp. 19572-19585, Jan. 2021, doi: 10.1109/ACCESS.2021.3055027.
- [8] S. Yachiangkam et al., "Wireless Golf Cart Charging Development in Thailand," *2022 International Electrical Engineering Congress (IEECON)*, Khon Kaen, Thailand, 2022, pp. 1-4, doi: 10.1109/IEECON53204.2022.9741670.
- [9] A. Mahesh, B. Chokkalingam, and L. Mihet-Popa,

"Inductive Wireless Power Transfer Charging for Electric Vehicles-A Review," *IEEE Access*, vol. 9, pp. 137667–137713, Sep. 2021, doi: 10.1109/ACCESS.2021.3116678.

[10] J. -J. Kao, C.-L. Lin and J. Yang, "Adaptive Wireless Power Transfer System With Relay Transmission and Communication," *IEEE Transactions on Power Electronics*, vol. 38, no. 3, pp. 4110-4123, March 2023, doi: 10.1109/TPEL.2022.3218368.

[11] SAE International, "J2954: Wireless power transfer for light-duty plugin/electric vehicles and alignment methodology," 2017.

[12] IEC Standards, *IEC 61980-1 Electric Vehicle Wireless Power Transfer (WPT) System – Part 1: General Requirements*, edition 1.0, International Standards, pp. 17, 2015.

[13] I. Casaucao, A. Triviño-Cabrera, and A. Delgado, "Ferromagnetic design of coils considering misalignment effects for a SAE J2954-compliant EV wireless charger," *IEEE Access*, p. 1, Jan. 2024, doi: 10.1109/access.2024.3492350.

[14] V. Cirimele, F. Freschi, and L. Zhao, "Critical comparative review of international standards on wireless charging for light-duty electric vehicles," *IEEE Transactions on Industry Applications*, pp. 1–10, Jan. 2024, doi: 10.1109/tia.2024.3408107.

[15] J. Zeng, J. Wu, K. Li, Y. Yang, and S. Y. R. Hui, "Dynamic Monitoring of Battery Variables and Mutual Inductance for Primary-Side Control of a Wireless Charging System," *IEEE Transactions on Industrial Electronics*, vol. 71, no. 7, pp. 7966-7974, July 2024, doi: 10.1109/TIE.2023.3312440.

[16] D. Patil, M. K. McDonough, J. M. Miller, B. Fahimi and P. T. Balsara, "Wireless Power Transfer for Vehicular Applications: Overview and Challenges," *IEEE Transactions on Transportation Electrification*, vol. 4, no. 1, pp. 3-37, March 2018, doi: 10.1109/TTE.2017.2780627.

[17] Y. Tian, Z. Li, H. Liu, Y. Liu and M. Ban, "High-Performance Wireless Charging System Using Interleaved Buck Converter and Integrated Solenoid Magnetic Coupler," in *IEEE Transactions on Transportation Electrification*, vol. 9, no. 3, pp. 3821-3835, Sept. 2023, doi: 10.1109/TTE.2023.3245087.

[18] H. -L. Jou, J. -C. Wu, K. -D. Wu and C. -Y. Kuo, "Bidirectional DC-DC Wireless Power Transfer Based on LCC-C Resonant Compensation," *IEEE Transactions on Power Electronics*, vol. 36, no. 2, pp. 2310-2319, Feb. 2021, doi: 10.1109/TPEL.2020.3005804.

[19] M. Kim, D. -M. Joo and B. K. Lee, "Design and Control of Inductive Power Transfer System for Electric Vehicles Considering Wide Variation of Output Voltage and Coupling Coefficient," *IEEE Transactions on Power Electronics*, vol. 34, no. 2, pp. 1197-1208, Feb. 2019, doi: 10.1109/TPEL.2018.2835161.

[20] J. M. González-González, A. Triviño-Cabrera, and J. A. Aguado, "Model Predictive Control to Maximize the Efficiency in EV Wireless Chargers," *IEEE Transactions on Industrial Electronics*, vol. 69, no. 2, pp. 1244-1253, Feb. 2022, doi: 10.1109/TIE.2021.3057006.

[21] A. Babaki, S. Vaez-Zadeh, A. Zakerian, and G. A. Covic, "Variable-Frequency Retuned WPT System for Power Transfer and Efficiency Improvement in Dynamic EV Charging With Fixed Voltage Characteristic," *IEEE Transactions on Energy Conversion*, vol. 36, no. 3, pp. 2141-2151, Sept. 2021, doi: 10.1109/TEC.2020.3048196.

[22] Lassioui, Abdellah, Marouane El Ancary, Zakariae El Idrissi, Hassan El Fadil, Kamal Rachid, and Aziz Rachid. 2024. "Primary-Side Indirect Control of the Battery Charging Current in a Wireless Power Transfer Charger Using Adaptive Hill-Climbing Control Technique" *Processes* 12, no. 6: 1264.

[23] G. R. Kalra, B. S. Riar and D. J. Thrimawithana, "An Integrated Boost Active Bridge Based Secondary Inductive Power Transfer Converter," *IEEE Transactions on Power Electronics*, vol. 35, no. 12, pp. 12716-12727, Dec. 2020, doi: 10.1109/TPEL.2020.2984784.

[24] J. Thongpron, et al., "A 10 kW Inductive Wireless Power Transfer Prototype for EV Charging in Thailand," *ECTI Transactions on Electrical Engineering, Electronics, and Communications*, vol. 20, no. 1, pp. 83-95, Feb 2022.

[25] T. Somsak, et al., "Constant Current - voltage with Maximum Efficiency Inductive Wireless EV Charging Control using Dual-sided DC Converters," *2021 18th International Conference on Electrical Engineering/Electronics, Computer, Telecommunications and Information Technology (ECTI-CON)*, Chiang Mai, Thailand, 2021, pp. 936-941, doi: 10.1109/ECTI-CON51831.2021.9454726.

[26] A. Namin, et al., "Solar Tricycle with Lateral Misalignment Maximum Power Point Tracking Wireless Power Transfer," *2018 15th International Conference on Electrical Engineering/Electronics, Computer, Telecommunications and Information Technology (ECTI-CON)*, Chiang Rai, Thailand, 2018, pp. 656-659, doi: 10.1109/ECTICon.2018.8619926.

[27] IEC, "IEC TS 61980-2: Electric Vehicle Wireless Power Transfer (WPT) – Part 2: Specific Requirement for Communication between Electric Road Vehicle (EV) and Infrastructure," IEC, Geneva, Switzerland, 2019, 85 p.

[28] IEC, "CISPR 11: Industrial, Scientific and Medical Equipment – Radio-frequency Disturbance Characteristics – Limits and Methods of Measurement," *International Electrotechnical Commission*, Geneva, Switzerland, 2021.

[29] IEC, "IEC TS 61980-3: Electric Vehicle Wireless Power Transfer (WPT) – Part 3: Specific Requirement for Magnetic Field Wireless Power Transfer System," IEC, Geneva, Switzerland, 2019, 107 p.

[30] S. Mueanggoen, and Y. Kumsuwan, "Essen-

tial Testing and Stepwise Evaluation of Lithium-Ion Battery Packs for Electric Vehicles," *ECTI Transactions on Electrical Engineering, Electronics, and Communications*, vol.23, no.2, 2025, <https://doi.org/10.37936/ecti-eec.2525232.259270>

[31] W. San-Um and T. Masayoshi, "An On-Chip Analog Mixed-Signal Testing Compliant with IEEE 1149.4 Standard Using Fault Signature Characterization Technique," *ECTI Transactions on Electrical Engineering, Electronics, and Communications*, vol. 8, no. 1, 2009, pp.85–92. <https://doi.org/10.37936/ecti-eec.201081.172036>.

[32] U. Kamnarn *et al.*, "CC–CV Wireless EV Charging With Power Balance Control in Primary- and Secondary-Side Converters," *IEEE Access*, vol. 13, pp. 151597–151613, 2025, doi: 10.1109/ACCESS.2025.3602478.

[33] A. Namin, C. Donloei, and E. Chaidee, "Wireless charging Class-E inverter for zero-voltage switching over coupling coefficient range," *International Journal of Power Electronics and Drive Systems (IJPEDS)*, vol. 16, no. 3, September 2025, pp. 1752-1764. doi: <http://doi.org/10.11591/ijpeds.v16.i3.pp1752-1764>.

[34] T. Singhavilai, *et al.*, "Evaluating Wireless Power Transfer Technologies for Electric Vehicles: Efficiency and Practical Implementation of Inductive, Capacitive, and Hybrid Systems," *IEEE Access*, vol. 13, pp. 9792-9808, 2025, doi: 10.1109/ACCESS.2025.3527122.



**Surasak Yousawat** is an Assistant Professor in the Department of Electrical Engineering, Rajamangala University of Technology Lanna (RMUTL), Chiang Mai, Thailand. He received the B.Eng. in Electrical Engineering from King Mongkut's Institute of Technology Thonburi, Bangkok, Thailand, in 1993. His M.Eng. in Electrical Engineering in Chiang Mai University (CMU), Thailand, in 1999. His main research interests include power electronics and control, engineering education didactics, etc.



**Ekkachai Chaidee** is an Assistant Professor in the Department of Electrical Engineering, Rajamangala University of Technology Lanna (RMUTL), Chiang Rai, Thailand. He received the B.S. Ind. Ed. in Electrical engineering from the King Mongkut's University of Technology Thonburi (KMUTT), Bangkok, Thailand, in 2001 and the M.Sc. Eng. in Electrical Engineering from the King Mongkut's University of Technology North Bangkok (KMUTNB), Bangkok, Thailand, in 2008. He is finished the D.Eng. in Electrical and Information Engineering Technology from King Mongkut's University of Technology Thonburi (KMUTT) in 2022. His main research interests include power electronics and inductive wireless power transfer.



**Wuttikai Tammawan** is a Lecturer of Rajamangala University of Technology Lanna (RMUTL), Chiang Rai, Thailand. He received the B.Eng. in Electrical Engineering from Rajamangala University of Technology Lanna, Chiang Rai, Thailand, in 2019. His M.Eng. in Electrical Engineering from Rajamangala University of Technology Lanna, Chiang Mai, Thailand, in 2023. His research interests include wireless power transfer, inductive wireless power transfer, power electronics, wireless EV chargers, etc.



**Thanet Sriprom** is a D. Eng. student of Rajamangala University of Technology Lanna (RMUTL), Chiang Rai, Thailand. He received the B. Eng. and M. Eng. in Electrical Engineering from Rajamangala University of Technology Lanna, Thailand in 2016 and 2023 respectively. His main research interests include power electronic circuits and control, inductive wireless power transfer, power balance controller, Hamiltonian control for buck-converter in wireless power transfer system, etc.



**Worrajak Muangjai** is an Assistant Professor in the Department of Electrical Engineering, Rajamangala University of Technology Lanna, Chiang Mai, Thailand. He received a B.S. Tech. Ed. in Electrical Engineering in 1996 from Rajamangala Institute of Technology, Chiang Mai Campus, M.Eng. and Ph.D. in Electrical Engineering from Chiang Mai University in 2007 and 2016, respectively. His main research areas are Microcontrollers, IoT, Power Electronics, and Renewable Energy, etc.



**Nopporn Patcharapakiti** is an Assistant Professor in Electrical Engineering, Faculty of Engineering at Rajamangala University of Technology Lanna (RMUTL), Chiang Mai, Thailand. He received the B.Eng. and M.Eng. degrees in Electrical Engineering from Chiang Mai University, Chiang Mai, Thailand. He also received the Ph.D. degree in Energy Technology from King Mongkut's University of Technology Thonburi (KMUTT), Bangkok, Thailand. His research interests include

Power Systems, Renewable Energy, Photovoltaic Systems and Grid-Connected Inverters, Electric Vehicles and Vehicle-to-Grid (V2G), System Identification and Modeling.



**Jutturit Thongpron** is an Associate Professor in the Department of Electrical Engineering, Faculty of Engineering, Rajamangala University of Technology Lanna, Chiang Mai, Thailand. He received his B.S.Tech.Ed. and M.S.Tech.Ed. in Electrical Engineering from King Mongkut's University of Technology North Bangkok (KMUTNB) in 1990 and 1994, respectively. His D.Eng. in Energy Technology was completed from King Mongkut's University of Technology Thonburi (KMUTT) in 2005. His primary research interests are in photovoltaic characterization and applications, smart grid technology, inductive wireless power transfer, wireless EV charging stations, and electrical engineering education.



**Anon Namin** is an Assistant Professor in the Department of Electrical Engineering, Rajamangala University of Technology Lanna (RMUTL), Chiang Mai, Thailand. He received the B.Sc.Ind.Ed. in Electrical Engineering from King Mongkut's Institute of Technology Thonburi, Bangkok, Thailand, in 1996. His M.Sc.Ind.Ed. in Electrical Engineering and Ph.D. in Energy Technology are finished from King Mongkut's Institute of Technology Thonburi (KMUTT), Thailand, in 2002 and 2013, respectively. His main research interests include the field of power electronic circuits and control, inductive wireless power transfer, PV characterization using solar simulator, and electrical engineering education. etc.